

# Evaluation of thermo-mechanical damage and fatigue life of solar cell solder interconnections

Musa T. Zarmai\*, N.N. Ekere, C.F. Oduoza, Emeka H. Amalu  
School of Engineering, Faculty of Science and Engineering,  
University of Wolverhampton, Wolverhampton, WV1 1LY, UK

## Abstract

The soldering process of interconnecting crystalline silicon solar cells to form photovoltaic (PV) module is a key manufacturing process. However, during the soldering process, stress is induced in the solar cell solder joints and remains in the joint as residual stress after soldering. Furthermore, during the module service life time, thermo-mechanical degradation of the solder joints occurs due to thermal cycling of the joints which induce stress, creep strain and strain energy. The resultant effect of damage on the solder joint is premature failure, hence shortened fatigue life. This study seeks to determine accumulated thermo-mechanical damage and fatigue life of solder interconnection in solar cell assembly under thermo-mechanical cycling conditions. In this investigation, finite element modelling (FEM) and simulations are carried out in order to determine nonlinear degradation of SnAgCu solder joints. The degradation of the solder material is simulated using Garofalo-Arrhenius creep model. A three dimensional (3D) geometric model is subjected to six accelerated thermal cycles (ATCs) utilising IEC 61215 standard for photovoltaic panels. The results demonstrate that induced stress, strain and strain energy impacts the solder joints during operations. Furthermore, the larger the accumulated creep strain and creep strain energy in the joints, the shorter the fatigue life. This indicates that creep strain and creep strain energy in the solder joints significantly impacts the thermo-mechanical reliability of the assembly joints. Regions of solder joint with critical stress, strain and strain energy values including their distribution are determined. Analysis of results demonstrates that creep energy density is a better parameter than creep strain in predicting interconnection fatigue life. The use of six ATCs yields significant data which enable better understanding of the response of the solder joints to the induced loads. Moreover, information obtained from this study can be used for improved design and better-quality fabrication of solder interconnections in solar cell assembly for enhanced thermo-mechanical reliability.

**Keywords:** PV manufacturing, crystalline silicon solar cell, solder joint, thermo-mechanical damage, fatigue life

## 1. Introduction

Crystalline silicon solar cells are the most common and widely used solar cells with a production history of over 60 years. The global capacity for production of this solar cell is high and also delivers the highest efficiencies of energy conversion. Silicon is the primary feedstock used in the fabrication of crystalline silicon wafers for use in making the solar cells. Solders are employed as interconnection materials for soldering silver (Ag) busbar on silicon wafer to copper (Cu) ribbon strip in crystalline silicon solar cell assemblies in order to form a

photovoltaic (PV) module. Conventional PV modules are designed and manufactured for a lifespan of about 25 years. Though interconnection of solar cells can be carried out manually, automated machinery known as stringers are also used. Some typical stringers used in interconnecting solar cells are presented in Fig.1. They are usually designed for a specific soldering technology such as infrared soldering, laser soldering or any desired soldering technology.

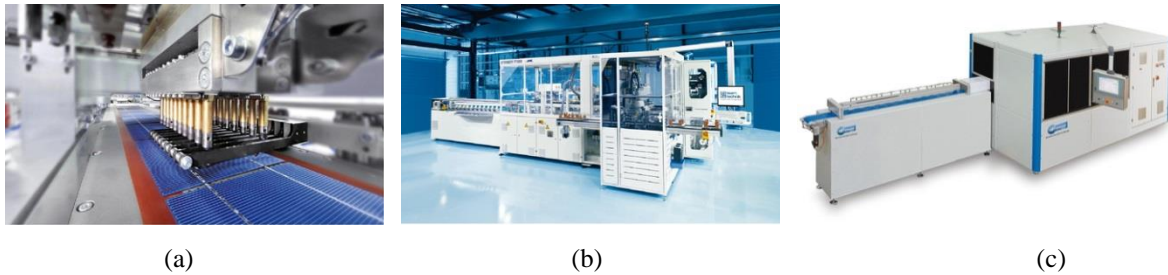


**Fig. 1.** Typical stringers used in interconnecting solar cells [1]  
(a) IMA’s modustringer system  
(b) Teamtechnik’s stringer TT1200 single track system  
(c) P.energy’s stringer system

Several soldering processes can be used to solder Ag busbar to Cu ribbon strip as mentioned earlier. These processes can be manual processing, semi-automated processing and full automated processing which can include the use of robots. The use of robots in PV manufacturing provides the benefits of increased quality due to good solder joint formation as well as reduced cost of soldering the solar cells. Figure 2 show a robot effector with soldering heads and vacuum pick-up arm used for interconnecting solar cells while Fig. 3 shows a slide-mounted solder head suspended from robot arm. Both the robot effector and solder head in Figs. 2 and 3 respectively are products of Spire Corporation, which is a Massachusetts, US based PV equipment manufacturer.

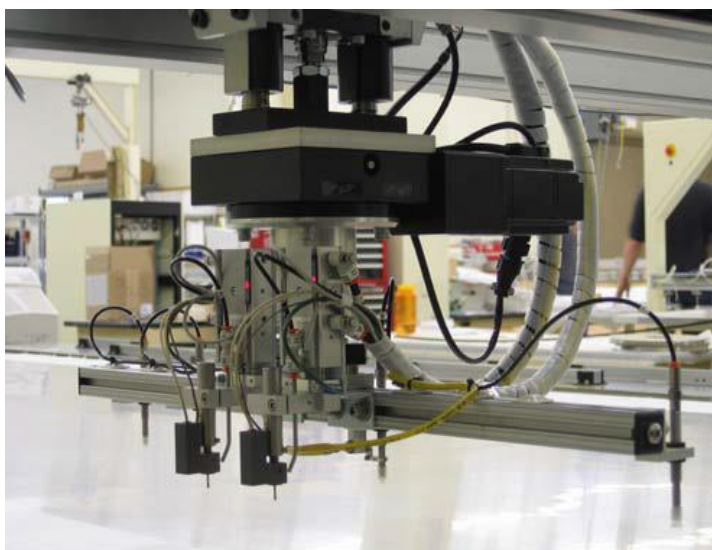


**Fig. 2.** Spire robot end effector with soldering heads and vacuum pick-up for interconnecting solar cells [2]

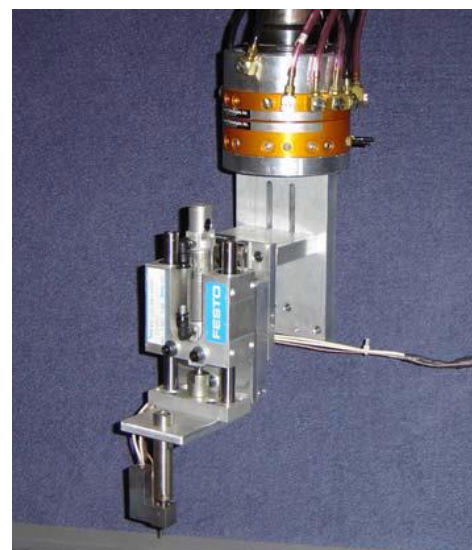


**Fig. 3.** Spire slide-mounted solder head suspended from robot arm [2]

Irrespective of the soldering process used to form solder joints in the PV module, the primary function of the joints is to act as mechanical support to hold the ribbon strip to the silicon wafer via silver busbar. They also function as thermal conduit for heat dissipation away from the silicon wafer as well as providing the critical electrical interconnection between the silicon wafer and the copper ribbon.

However, regardless of technique and machinery used in soldering solar cells, solder joint long-term reliability throughout the PV module lifetime is a key concern. One of the effects of soldering is that stress is induced in the solar cell solder joint during soldering and remains in the joint as residual stress after soldering. Moreover, solder materials in solar cell assemblies are subjected to thermo-mechanical loads during accelerated thermal cycling tests as well as in service operation and can result in thermal fatigue failure of the solder joint [3]. The mismatch of coefficient of thermal expansion (CTE) of silicon wafer, silver busbar, solder, copper ribbon strip and other components, leads to thermo-mechanical induced non-linear deformation in the solar cell assembly. The induced deformations in the solar cell assembly cause the solder materials to develop cyclic inelastic plastic and creep strains which cause cumulative fatigue damage resulting in failure of the solder joints [4, 5]. This occurs when the cyclic strain increases to a particular high value and the ensuing damage in the solder material cause fatigue cracking in the solder joints thereby resulting in premature failure of the PV module's functional life [5]. Creep of a solder material is often characterized by its steady state creep strain rate [4]. According to Che and Pang [6], the steady state creep model of solder is of major concern due to its contribution to total creep deformation. Therefore, an investigation of steady state creep for non-linear deformation of SnAgCu solder joints in crystalline silicon solar cell assembly is needed to obtain more understanding. In this study, 95.5Sn-3.8Ag-0.7Cu lead-free (Pb-free) solder alloy is used.

This study employs finite element modelling (FEM) to simulate the nonlinear deformation of SnAgCu solder joints in a model of crystalline silicon solar cell assembly. The Garofalo-Arrhenius steady state creep constitutive model for SnAgCu solder will be used in this study to simulate the degradation of solder material.

## **2. Solar cell assembly and reliability**

The architecture of solar cell assembly used in this research and a brief overview of solder joint reliability are presented in two parts.

### **2.1 Architecture of solar cell assembly**

The manufacturing process of conventional wafer-based crystalline solar cells begins with the use of silicon wafer as a base. A layer of emitter material is deposited on this base on which a layer of an anti-reflection coating (ARC) is in turn deposited on. The ARC layer ensures passage of all light to the silicon crystalline layers while minimizing reflection. A transparent adhesive is deposited on the overlaid coating. Two layers of silver in grid form are then printed on the cell's semiconductor material such that the metallization penetrates the ARC layer and makes contact with silicon wafer to form the front metal contact and collect electric current generated. The printed contacts are fired. Typically, aluminium contacts are also printed at the back surfaces of the cell material. A typical Schematic of cross-section of a laminated crystalline Si solar cell is depicted in Fig. 4 and consists basically of material layers. As can be observed from the figure, a rear contact material supports silicon wafer. The

silicon wafer serves as a semiconductor consisting of a P-type layer at the rear and an N-type layer on the front. This layer is secured by a protective glass cover [7]. Solar cells are interconnected with other cells in series and parallel to form a PV module of the required voltage and current. However, it should be noted that the coefficient of thermal expansion (CTE) of the copper ribbon, solder alloy and silver busbar are different. The CTE mismatch induce thermo-mechanical stresses in the solder joint during soldering as well as service operations resulting in fatigue and eventual failure. It is desirable that the packaging of the PV module should ensure the solder joint maintains integrity and reliability through subsequent manufacturing processes as well as during service conditions. Presented in Fig. 5 is a schematic of crystalline silicon solar cells interconnected in series with tabbing ribbon.

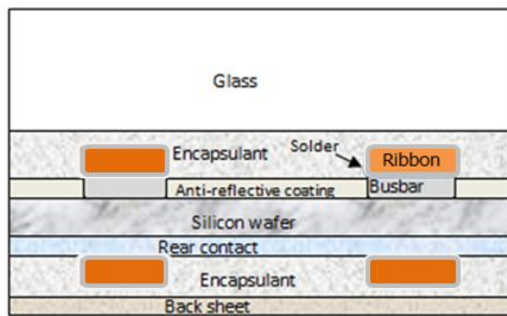


**Fig. 4.** Schematic of cross-section of a typical laminated crystalline Si solar cell

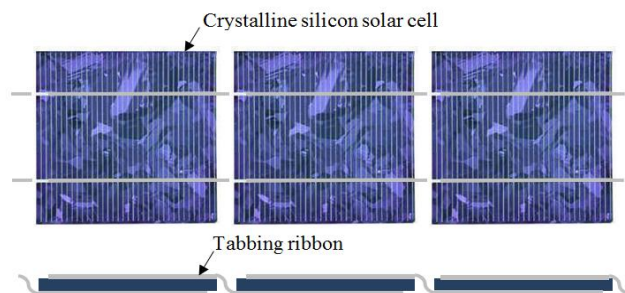


**Fig. 5.** Crystalline silicon solar cells interconnected in series with tabbing ribbon

## 2.2 Solder joint reliability

In order to interconnect solar cells, printed contacts at the front and back surfaces of the cells are soldered to highly conductive ribbon strips for current transfer from the front of one cell to the back of a neighbouring cell in a series connection [8] as shown in Fig. 5. The reliability of solder joints can be affected by a variety of application conditions such as vibration, mechanical shock, thermo-mechanical fatigue, thermal aging and humidity [9]. McCluskey [10] and Cuddalorepatta, et al [11] reported that the soldered interconnect joint is the most susceptible part of the assembly. Moreover, in a BP Solar study of PV module field failures, Wohlgemuth [12] reported that cell/interconnect break accounted for 40.7% of all types of field failures observed. The substantial failure of interconnects demonstrate their crucial role and the need to provide urgent solution to this critical challenge. This study is focussed on the thermo-mechanical reliability of solder joints in crystalline silicon PV modules.

## 3. FE modelling and simulation

This section discusses the study of thermo-mechanical reliability of solder joints in solar cell assembly subjected to thermal cycling using finite element modelling (FEM).

### 3.1 Background and methodology

The study of induced strain in solar cell assembly was carried out using commercial ANSYS academic research finite element package. A dedicated Work Station Server was used to execute the High Performance Computation (HPC) due to the huge magnitude of computations involved in the modelling and simulation. In order to reduce computation

resources and time, a quarter symmetry of the geometric model of standard 156mm × 156mm multi-crystalline silicon solar cell assembly was used in this study. Presented in Fig. 6(a) is the meshed geometric model of the whole assembly of crystalline silicon solar cell while Fig. 6(b) shows the section of the model where components are interconnected.

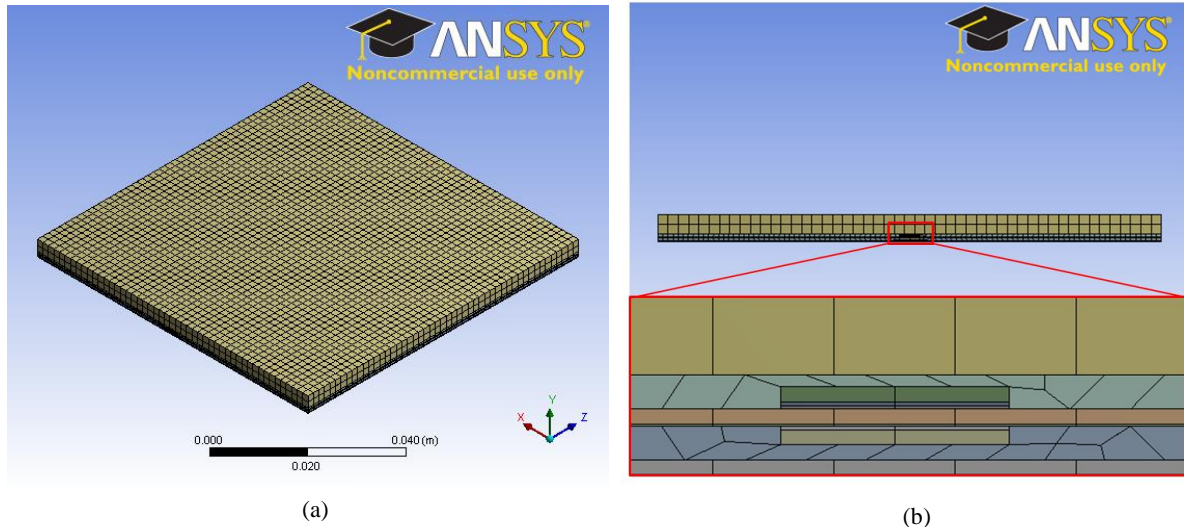


**Fig. 6.** Crystalline silicon solar cell assembly showing: (a) the meshed assembly and (b) interconnected components

### 3.2 Materials and their properties

An observation of the solar cell schematic cross-section presented in Fig. 4 shows that the solar cell assembly consists of various materials with dissimilar properties. These materials and their corresponding properties were used to build the geometric models for this study. The properties of these materials are presented in Table 1. The Sn-3.8Ag-0.7Cu solder material in solar cell assembly is interconnected with the copper ribbon at the upper interface of the assembly while at the lower interface it is interconnected with Ag busbar. It can be observed from Table 1 that the coefficient of thermal expansion of the solder, Cu ribbon and Ag busbar are all different from each other. Thus during thermal cycling, expansion and contraction of these materials readily ensue.

**Table 1:** Mechanical properties of materials in solar cell assembly

Component	Young modulus (GPa) E	CTE ( $10^{-6}/^{\circ}\text{C}$ ) $\alpha$	Poisson's ratio $\nu$	Shear modulus (GPa) G
Glass [13]	73.3	8.5	0.21	30.289
Eva encapsulant [14]	0.011	270	0.4999	0.00367
Cu ribbon [15, 16]	129	17	0.34	48.134
Solder (Sn3.8Ag0.7Cu) [16]	43	23.2	0.3	16.538
Ag busbar [17]	7	10.4	0.37	2.5547
Si wafer [18]	130	3.5	0.22	53.279
Al rear contact [19]	6	11.9	0.33	2.2556
Tedlar back sheet [20]	1.4	30	0.4	0.5

### 3.2.1 Constitutive solder model

Solder joints in solar cell assemblies undergo thermo-mechanical loading during accelerated thermal cycling tests as well as in field service. The elastic and inelastic deformation behaviour of the solder alloy is described by constitutive models. One of the solder constitutive models commonly used in finite element analysis (FEA) is the Garofalo-Arrhenius creep model. Creep of a solder material is often characterized by its steady-state creep strain rate [4]. The solder is assumed to exhibit elastic, bilinear kinematic hardening after yield.

In this study, the hyperbolic sine creep equation was used to simulate the creep behaviour of Sn-3.8Ag-0.7Cu solder joints. The steady state creep strain rate is given by [21]:

$$\dot{\epsilon}_{cr} = A_1 [\sinh(\alpha\sigma)]^n \exp\left(\frac{-H_1}{kT}\right) \quad (1)$$

This equation is then re-written into equation (2) in the required format of input for implicit Garofalo-Arrhenius creep model:

$$\dot{\epsilon}_{cr} = C_1 [\sinh(C_2\sigma)]^{C_3} \exp^{-C_4/T} \quad (2)$$

The constants  $C_1$ ,  $C_2$ ,  $C_3$  and  $C_4$  are parameters for Sn-3.8Ag-0.7Cu solder and are presented in the Table 2:

**Table 2:** Garofalo creep parameters for Sn-3.8Ag-0.7Cu solder [21]

Parameter	$C_1$ (1/s)	$C_2$ (MPa) <sup>-1</sup>	$C_3$	$C_4$ (K)
Value	2.7798E+05	2.447E-02	6.41	6500

### 3.2.2 Fatigue life prediction model

The fatigue life of solder subjected to thermal cycling is usually predicted using fatigue life prediction models such as hyperbolic sine constitutive equation. The constitutive equation is a damage mechanism-based life prediction model. The primary damage mechanism for SnAgCu solder during thermal cycling is creep and it is used to simulate the material behaviour. Therefore, the life prediction model has to be theoretically based on creep deformation [21].

The accumulated creep strain and accumulated creep strain energy density per cycle are presented below and used to predict fatigue life of solder joints subjected to thermal cycling loading.

Accumulated creep strain is given by:

$$N_f = (C' \epsilon_{acc})^{-1} \quad (3)$$

Accumulated creep energy density per cycle is given by:

$$N_f = (W'w_{acc})^{-1} \quad (4)$$

where,  $N_f$  = Number of repetitions or cycles to failure.

$\epsilon_{acc}$  = Accumulated creep strain per cycle.

$C' = 1/\epsilon_f$ , inverse of creep ductility.

$W'$  = Creep energy density for failure.

$w_{acc}$  = Accumulated creep energy density per cycle.

The value of the accumulated creep strain induced or accumulated creep energy density per cycle in a solder joint is calculated and used to determine the number of cycles to failure. The constants  $C'$  and  $W'$  have been experimentally determined to be 0.0513 and 0.0019 respectively [21].

### 3.3 Loads and boundary conditions

The geometric models were subjected to six accelerated thermal cycling in 25 load steps between  $-40\text{ }^\circ\text{C}$  to  $85\text{ }^\circ\text{C}$  utilising IEC 61215 standard for photovoltaic panels. The temperature loading started from  $25\text{ }^\circ\text{C}$ , ramped up at a rate of  $3\text{ }^\circ\text{C}/\text{min}$  to  $85\text{ }^\circ\text{C}$ , where it had hot dwell for 20 min. It was then ramped down to  $-40\text{ }^\circ\text{C}$  at a rate of  $6\text{ }^\circ\text{C}/\text{min}$ , where it had cold dwell for 20 min. Presented in Fig. 7 is the thermal cycling profile used for simulation. This thermal cycling profile is used to accurately simulate actual cycling profile used during thermal load test.

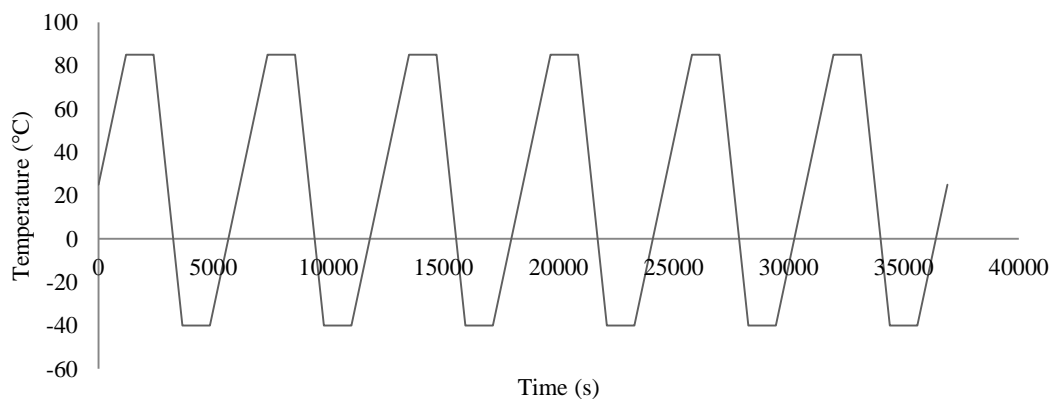


Fig. 7. Plot of temperature profile of thermal load test condition used in the solar cell

## 4. Results and discussion

The results obtained from the modelling and simulation are analysed and discussed in six parts.

### 4.1 Study on creep strain

One of the aims of simulating thermo-mechanical loading of solder joint in solar cell assembly is to obtain creep deformation behaviour of the SnAgCu solder material. The creep response of the solder joint in the solar cell assembly to thermal load is captured as damage distribution of the accumulated stress, strain and strain energy in the joint. The representation

of the stress, strain and strain energy damage distribution for the top layer of solder is shown in Fig. 8. Figure 8(a) shows that the solder joint has minimal strain at the two ends of the solder joint and it increases along the longitudinal axis to the middle section of the joint. The induced creep strain can lead to failure of solder joint and ultimately failure of the solar cell assembly to deliver power generated. Figure 9 shows the plot of equivalent creep strain against thermal cycle in solder layer and it indicates that as thermal cycling increases, the creep strain increases as well. This signifies that as the daily service operations of the PV modules continues, the solder joint in solar cell assembly becomes increasingly and detrimentally strained leading to crack initiation. Further daily thermal cycling results in crack propagation and finally fracture of the solder joint.

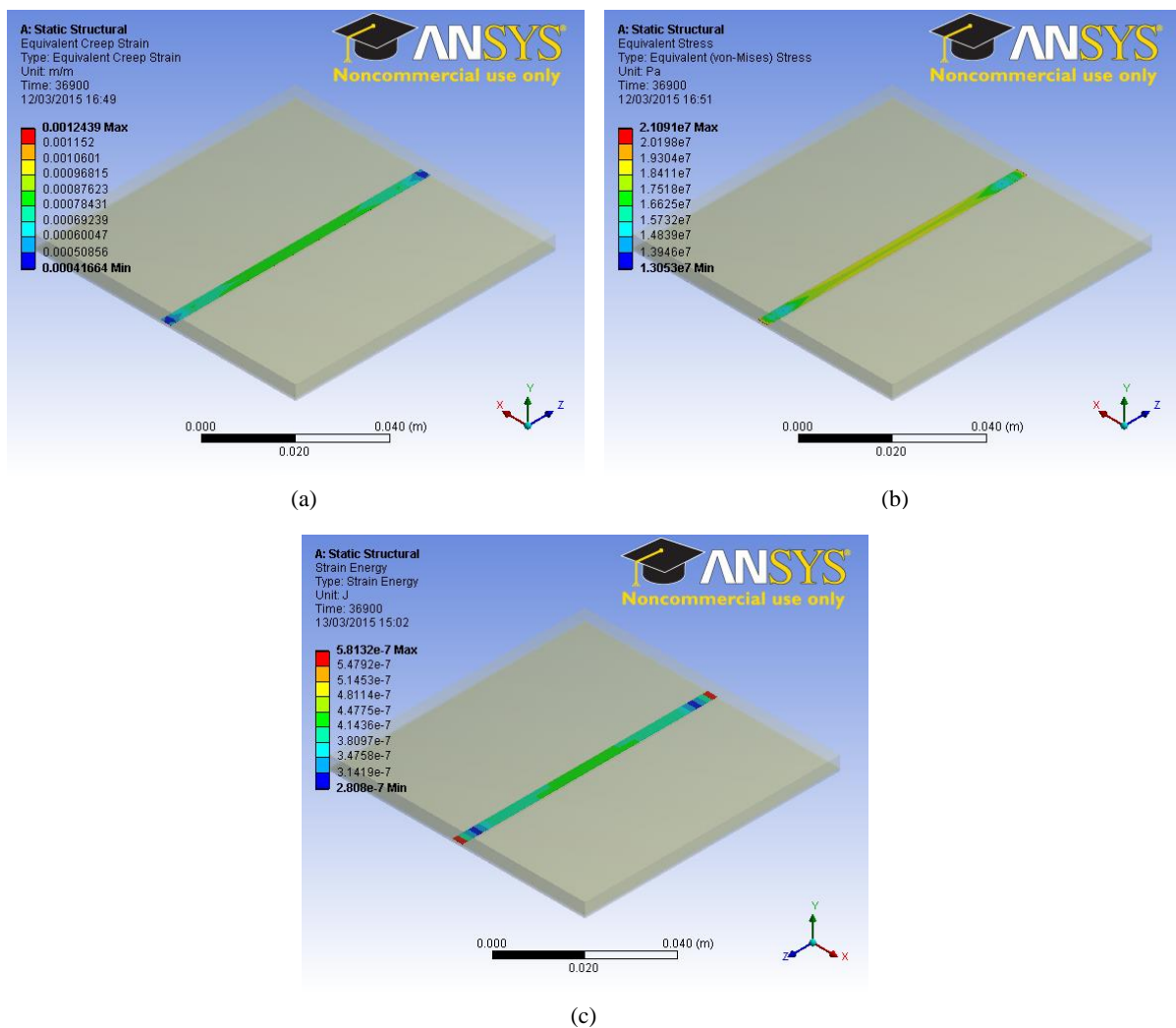


**Fig. 8.** Damage distribution solder joints of solar cell assembly showing:  
 (a) Equivalent creep strain (b) Equivalent stress (c) Strain energy



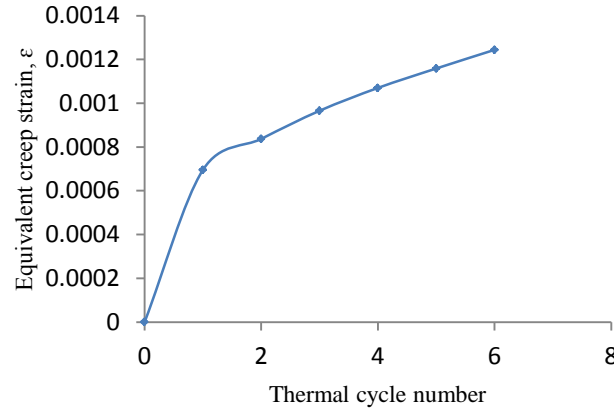


**Fig. 9.** Plot of Equivalent creep strain against thermal cycle in solder layer

## 4.2 Study on equivalent stress

A close observation and analysis of Fig. 8(b) shows that the solder joint has maximum stress concentration along longitudinal axis towards the two ends of the joint. Simulation results indicate a maximum induced stress of 21.091MPa in the solder joint. The induced stress in the solder joint significantly impacts the thermo-mechanical reliability of the solar cell assembly joints eventually resulting in failure of the joints. Presented in Fig. 10 are stress magnitudes and amplitudes of solar cell solder joint which are plotted using read out data points at the end of each thermal cycling load step. The plot shows that the stress magnitudes gradually increases at the commencement of thermal cycling and reaches a maximum after load step 17. The stress magnitude then decreases to a minimum value before increasing again to a high value after load step 23 followed by another final decrease to a minimum value at load step 25 which the last load step. Similarly, the stress amplitudes gradually increase at the commencement of the thermal cycling, reaches a maximum and decreases by the end of the last load step.

Considering that the solder joint has a Cu/solder/Ag sandwich structure, a close observation of Fig. 8(b) shows that equivalent stress damage distribution is higher at the lower interface of the solder layer which connects the Ag bus-bar, compared to the upper interface which connects the copper ribbon. This is not surprising considering that the difference in CTE of solder and Ag bus-bar is larger than that of solder and copper. Hence the CTE mismatch facilitates greater stress induction at the bonded interface with Ag bus-bar during thermal cycling. Thus, damage distribution gradients in the solder layer caused by differential thermal expansion of the solder constituents are more severe at this interface. This implies that this section of the solder interconnection is a critical failure site where crack initiation and propagation is most likely to begin. This observation agrees with the experimental observation by Schmitt et al [22] whose result showed greater solder joint degradation at the solder/Ag interface.

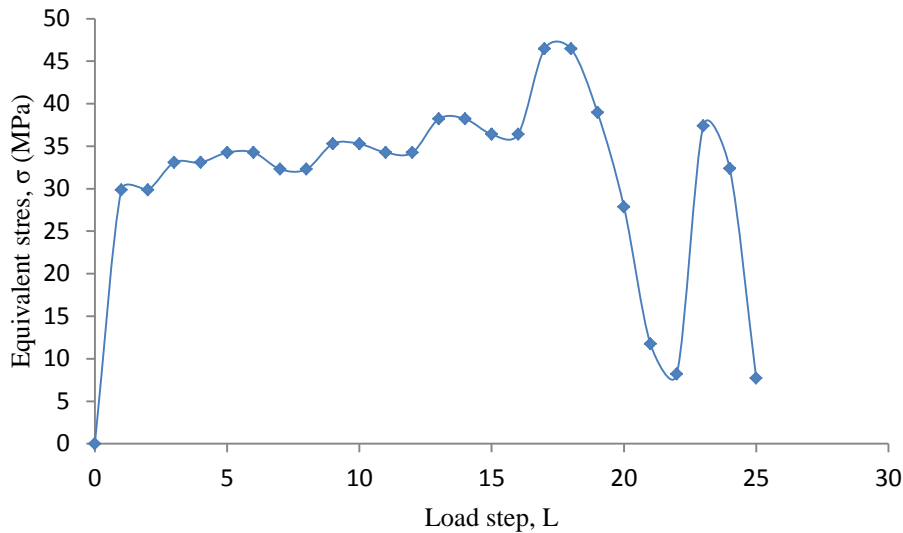


**Fig. 10.** Plot of equivalent stress on solder joint against load

### 4.3 Study on hysteresis

Figure 11 shows the hysteresis loop of solder for six thermal cycles which was plotted using equivalent creep strain and stress. The plot shows a steep rise in the trend as thermal cycling commences and continues up to a maximum value and then makes a transition with rapid decline followed by a slight constant state before another decline. Eventually, the trend rises again and forms a loop at the end of the first cycle. The rapid decline in stress magnitude indicates stress relaxation. A similar trend forms five other loops for each of the other five thermal cycles. It can be observed in the plot of Fig. 11 and Fig. 12 that under constant applied stress, the creep strain during the sixth thermal cycling increased up to a value of about 0.0022.

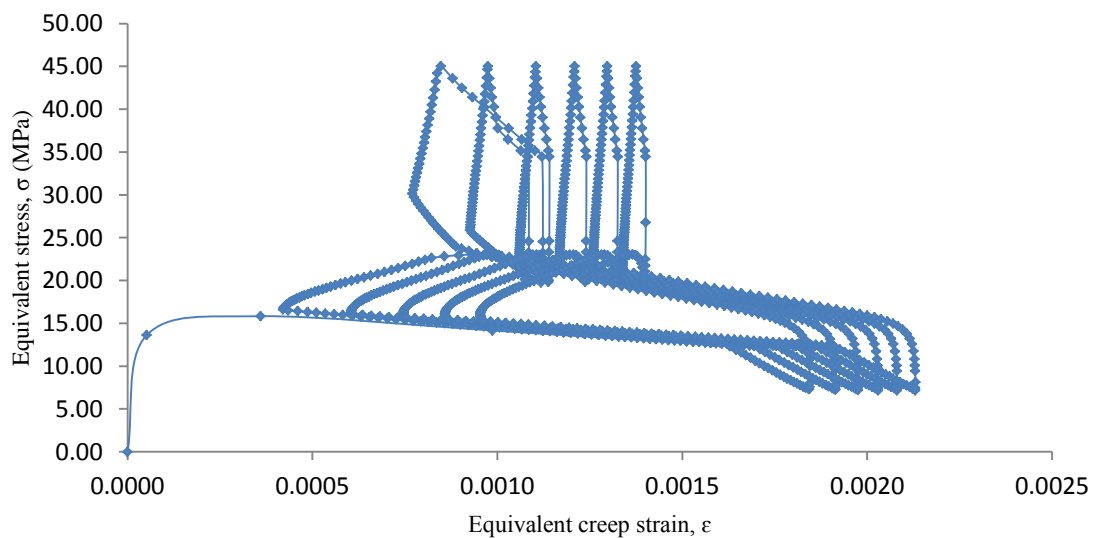


**Fig. 11.** Plot of hysteresis loop of solder joint

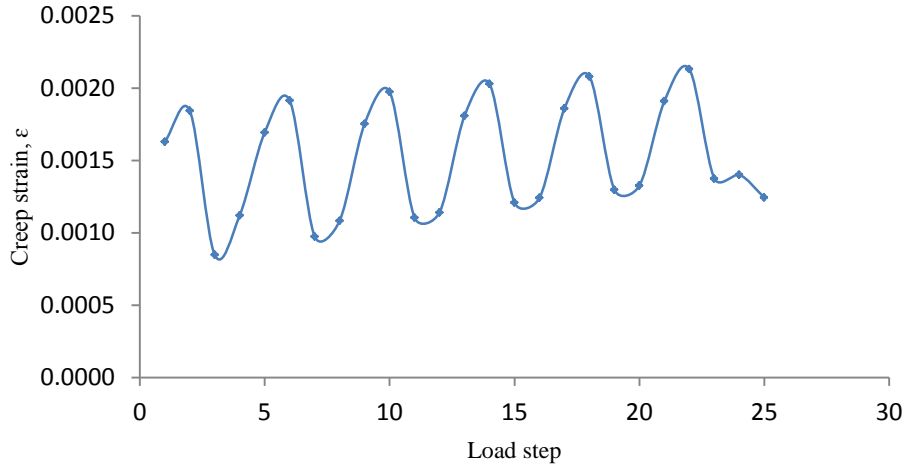


**Fig. 12.** Plot of equivalent creep strain on solder against load

#### 4.4 Study on creep strain energy

Creep strain energy in solder joint is the deformation in the joint caused by externally applied thermal load while the strain energy per unit volume is stated as strain energy density. A close observation of Fig. 8(c) shows regions of concern on the longitudinal axis, towards the two ends of the solder layer. Simulation results indicate maximum accumulated strain energy of 5.8132E-07J in the solder joint. In Fig. 13, a plot of creep strain energy against thermal cycle in solder layer is presented showing the strain energy declines slightly from the first thermal cycle to the last. As in the case of induced creep strain, accumulated creep strain energy in the solder joint can lead to its failure and ultimate failure of the solar cell assembly.

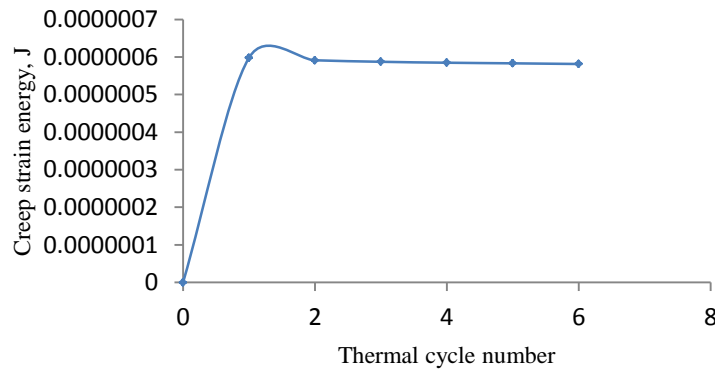


**Fig. 13.** Plot of Creep strain energy against thermal cycle in solder layer

#### 4.5 Solder joint fatigue life prediction

The solder joint service life can be predicted using the number of cycles to failure as proposed by Syed and presented in sub-section 3.2.2. Using the data used to plot Fig. 11, value of accumulated creep strain,  $\epsilon_{acc}$  is obtained as 0.0030535 and the number of cycles to failure is computed to be 6383. Similarly, from the data used to plot Fig. 11, the accumulated creep energy density,  $W_{acc}$  is obtained as 0.04754 mJ/mm<sup>3</sup> and the number of

cycles to failure is 11071. From the two values of number of cycles to failure, it can be observed that the value obtained through accumulated creep energy density is higher than the value obtained through creep strain. This is in line with computations by Syed [21]. Furthermore, the values are within the range of 6259 to 152464 cycles of failure obtained by Park et al [23].

#### 4.6 Discussion

The manufacturing of PV modules involves the interconnection of solar cells to each other through the soldering of copper ribbons as explained in section 2.1. This manufacturing process induces stress in the solder joint which is stored as residual stress. Furthermore, during the operation of the PV modules, the solder joints are subjected to thermo-mechanical fatigue loading due to thermal cycling and differences in the coefficient of thermal expansion (CTE) of the interconnect materials. Moreover, the fatigue loading creates creep deformation in the solder joint. The deformation is stored internally throughout the volume of solder joint as creep strain energy. Creep strain energy per unit volume of material is referred to as creep strain energy density. The degradation of the solder joints in the assembly are quantified using either accumulated creep strain or strain energy as the damage indices. Besides, as fatigue loading increases, more creep strain energy density accumulates in the solder joint. This eventually results in fatigue failure of the solder joints such that the larger the accumulated creep strain energy density, the shorter the fatigue life.

It was earlier stated in sub-section 3.2.2 that fatigue life is measured in number of repetitions or cycles to failure. In that regard, Guyenot et al. [24] estimated that for 1.5 thermal cycles per day with a temperature change of about 50 °C, expected life of solder joints in PV modules designed to last for 25 years is 13688 cycles to failure. On the other hand, Kohl et al. [25] in SunPower [26] reported that in a German four-year project, a group of PV modules from 7 different manufacturers were subjected to damp heat ageing test. The outcome of the test revealed significant performance degradation such that projected lifetime was less than 20 years (10950 cycles to failure). Likewise, Kumar and Sarkar [27] conducted a single constant stress accelerated life test on 20 PV modules for stress failure and obtained the least survival life to be 21 years (11497 cycles to failure). Table 3 presents predicted solder joint fatigue life of model compared with the expected life determined by Guyenot et al. [24] as well as test lives obtained by Kohl et al. [25] and that of Kumar and Sarkar [27].

**Table 3:** Predicted solar joint fatigue life of model compared with test results

Accumulated creep strain (cycles to failure)	Accumulated creep strain energy density (cycles to failure)	Expected test life [24] (cycles to failure)	Ageing test life [25] (cycles to failure)	Accelerated test life [27] (cycles to failure)
6383	11071	13688	10950	11497

An observation of values in Table 3 indicates that fatigue life of the geometric model under consideration obtained from the use of accumulated creep strain energy is well within the range when compared with test results. Moreover, the results of the computation of fatigue life of the solder joints using Eqns. 3 and 4 shows that the utilization of creep strain energy and its corresponding model produces a better result than creep strain and its model.

## 5. Conclusions

Study of the thermo-mechanical reliability of solder joints in crystalline silicon solar cell assembly was conducted using finite element analysis. Accumulated creep strain and strain energy are used as the damage indices to quantify the degradation of the solder joints in the assembly. The results show damage distribution gradients in the solder layer which would have been caused by differential thermal expansion of the solder constituents. This occurrence could lead to grain coarsening of solder particles and boundary sliding in the solder morphology. In long operations, the critical areas initiate cracks which could traverse the interconnection and cause module failure.

Formation of complete hysteresis loop up to the sixth thermal cycles supports earlier finding reported by Amalu and Ekere [28] and thus the authors emphasise the use of at least six temperature cycles in thermo-mechanical investigation of solder joints in not only electronic assemblies but also in photovoltaic modules. The results of the computation of fatigue life of the solder joints using the two relations demonstrates that the employment of creep strain energy and the model based on it give a better result than creep strain and its model. The authors suggest that PV manufacturers may adopt the least-stress inducing process when soldering solar cells in order to ensure improved fatigue life of solder joints. In addition, the information contained in this study can be utilized by PV manufacturers to improve the design and fabrication of solder interconnections in crystalline silicon solar cell assembly for enhanced thermo-mechanical reliability of the modules.

## Acknowledgements

The authors acknowledge funding provided by the Petroleum Technology Development Fund (PTDF), Nigeria used in carrying out this PG research work.

## References

- [1] Steinkötter, M. Reinventing stringers. PV Magazine; <<http://www.pv-magazine.com/archive/articles/beitrag/reinventing-stringers-100003049/329/#axzz3p2aTGxoA>>; 2011 [accessed 19.10.15].
- [2] Nowlan, M. Development of Automated Production Line Processes for Solar Brightfield Modules – subcontract report. Golden (Colorado): National Renewable Energy Laboratory Report: 2008. p. 1-101.
- [3] Che FX, Pang JHL. Characterization of IMC layer and its effect on thermo-mechanical fatigue life of Sn–3.8Ag–0.7Cu solder joints. *Journal of Alloys and Compounds*; 2012. 541:6-13.
- [4] Pang JHL. *Theory on Mechanics of Solder Material, Lead Free Solder: Mechanics and Reliability*. New York: Springer; 2012.
- [5] Hund T, Burchett SN. Solder fatigue reduction in point focus photovoltaic concentrator modules. In: 22<sup>nd</sup> IEEE Photovoltaic Specialists Conference, Las Vegas, NV; 1991. p. 754-79.
- [6] Che FX, Pang JHL. Thermal fatigue reliability analysis for PBGA with Sn-3.8Ag-0.7Cu solder joints. In: *Proceedings of 6th IEEE Electronics Packaging Technology Conference, Singapore*; 2004.

- [7] Dirjish M. What's The Difference Between Thin-Film And Crystalline-Silicon Solar Panels. In *Electronic Design eNewsletter*, Penton Media Inc.: New York, USA; 2012 p. 1-6.
- [8] Jeong J, Park N, Hong W, Han C. Analysis for the Degradation Mechanism of Photovoltaic Ribbon Wire under Thermal Cycling. In: *37<sup>th</sup> IEEE Photovoltaic Specialists Conference (PVSC)*, Seattle, WA; 2011. p. 003159-61.
- [9] Lechovič E, Hodúlová E, Szewczyková B, Kovaříková I, Ulrich K. Solder Joint Reliability;  
< [https://www.mtf.stuba.sk/docs/internetovy\\_casopis/2009/1/hodulova.pdf](https://www.mtf.stuba.sk/docs/internetovy_casopis/2009/1/hodulova.pdf)>; 2009 [accessed 12.03.13]. p. 1-8.
- [10] McCluskey FP. Reliability Modeling for Photovoltaic Modules. In: *Photovoltaic Module Reliability Workshop*, Denver, Colorado; 2010.
- [11] Cuddalorepatta G, Dasgupta A, Sealing S, Moyer J, Tolliver T, Loman J. Durability of Pb-free solder between copper interconnect and silicon in photovoltaic cells. *Progress in photovoltaics: research and applications* 2010; 18(3):168-82.
- [12] Wohlgemuth JH. Reliability of PV Systems. In: *Proceedings of SPIE: Reliability of Photovoltaic Cells, Modules, Components, and Systems*, SPIE Digital Library. 2008.
- [13] Webb JE, Hamilton JP. Physical Properties of Glass and the Requirements for Photovoltaic Modules. In: *Proceedings of Photovoltaic Module Reliability Workshop*, Golden, Colorado, USA; 2011. p. 1-18.
- [14] Eitner U, Pander M, Kajari-Schröder S, Köntges M, Altenbach H. Thermomechanics of PV Modules Including the Viscoelasticity of Eva. In: *26<sup>th</sup> Proceedings of European Photovoltaic Solar Energy Conference and Exhibition*, Hamburg, Germany; 2011. p. 3267-9.
- [15] Wiese S, Meier R, Kraemer F. Mechanical Behaviour and Fatigue of Copper Ribbons used as Solar Cell Interconnectors. In: *11<sup>th</sup> Proceedings of International Conference on Thermal, Mechanical and Multiphysics Simulation and Experiments in Micro-Electronics and Micro-Systems, EuroSimE*, Bordeaux, France; 2010.
- [16] Amalu EH, Ekere NN. High temperature reliability of lead-free solder joints in a flip chip assembly. *Journal of Materials Processing Technology* 2012; 212:471-83.
- [17] Wiese S, Meier R, Kraemer F, Bagdahn J. Constitutive Behaviour of Copper Ribbons used in Solar Cell Assembly Processes. In: *10<sup>th</sup> Proceedings of International Conference on Thermal, Mechanical and Multiphysics Simulation and Experiments in Micro-Electronics and Micro-Systems, EuroSimE*, Delft, The Netherlands; 2009.
- [18] Hopcroft MA, Nix WD, Kenny TW. What is the Young's Modulus of Silicon? *Journal of Microelectromechanical Systems* 2010; 19(2):229-38.
- [19] Wiese S, Kraemer F, Betzl N, Wald D. Interconnection Technologies for Photovoltaic Modules – Analysis of technological and mechanical Problems. In: *11<sup>th</sup> Proceedings of International Conference on Thermal, Mechanical and Multiphysics Simulation and Experiments in Micro-Electronics and Micro-Systems, EuroSimE*, Bordeaux, France; 2010.
- [20] Wiese S, Kraemer F, Peter E, Seib J. Mechanical Problems of novel Back Contact Solar Modules. In: *13<sup>th</sup> Proceedings of International Conference on Thermal Mechanical and Multi-Physics Simulation and Experiments in Microelectronics and Microsystems. EuroSimE*, Cascais, near Lisbon, Portugal; 2012.
- [21] Syed A. Accumulated Creep Strain and Energy Density Based Thermal Fatigue Life Prediction Models for SnAgCu Solder Joints. In: *54<sup>th</sup> Proceedings of Electronic Components and Technology Conference*, Las Vegas, USA; 2004. p. 737-46.
- [22] Schmitt P, Kaiser P, Savio C, Tranitz M, Eitner U. Intermetallic Phase Growth and Reliability of Sn-Ag- Soldered Solar Cell Joints. *Energy Procedia* 2012; 27:662-9.

- [23] Park N, Han C, Jeong J, Kim D. Lifetime Prediction Model of Thermal Fatigue Stress on Crystalline Silicon Photovoltaic Module. IEEE Transactions 2013; 1575-8.
- [24] Guyenot, M., Peter, E., Zerrer, P., Kraemer, F. and Wiese, S. (2011) Enhancing the lifetime prediction methodology for photovoltaic modules. Proceedings of 12th Int. Conf. on Thermal, Mechanical and Multiphysics Simulation and Experiments in Microelectronics and Microsystems. Linz, Austria, pp. 1-4.
- [25] Kohl, M., Weiss K., Heck, M. and Philipp, D. (2009) PV Reliability: Results of a German four-year joint project Part I: Accelerated ageing tests and modelling of degradation. 24th European Photovoltaic Solar Energy Conference and Exhibition. Hamburg, Germany. 21-25 September.
- [26] SunPower (2013) SunPower Module 40-year Useful Life. SunPower Corporation, USA. pp. 1-14.
- [27] Kumar, S. and Sarkar, B. (2013) Design for Reliability with Weibull Analysis for Photovoltaic Modules. International Journal of Current Engineering and Technology. 3(1), pp.129-134.
- [28] Amalu EH, Ekere NN. Prediction of damage and fatigue life of high-temperature flip chip assembly interconnections at operations. Microelectronics Reliability 2012; 52:2731-43.